Crystal Face Specificity of Electronic and Electrochemical Properties of a Neutral Interface: Analysis Using Density Functional Theory and the Bethe Approximation

R. Saradha and M. V. Sangaranarayanan*

Department of Chemistry, Indian Institute of Technology, Madras, Chennai-600 036, India

Received: December 2, 1997; In Final Form: February 16, 1998

A modified Jellium model, which includes the lattice effects in the form of Ashcroft pseudopotential, is analyzed using Smith's one-parameter family of trial function for electron-density profile, and work functions are calculated for various single crystals at the metal/vacuum interface. Face-dependent potential of zero charge (PZC) values for five sp metals are obtained by coupling the monolayer model of solvent dipoles with the modified Jellium model for the metal. The solvent molecules at the metal/solution interface are assigned two orientational states, and the dipolar interactions are treated using the Bethe approximation. A method of obtaining the work function, PZC, and surface potential for polycrystalline samples by suitably averaging over the single-crystal planes is outlined.

I. Introduction

The study of the electrode/electrolyte interface has been an area of extensive research activity during the past fifty years.[1] The continued interest in this topic is primarily due to the crucial role of the interfacial structure in all types of adsorption and charge transfer phenomena occurring at electrode surfaces and its influence on several technologically important processes such as electrocatalysis, electrodeposition, corrosion, and so forth. Inspite of such diverse attempts, the traditional analysis of interfacial structure (until the early 1980s) was based upon visualizing metals as perfect conductors,[2,3] the detailed electronic properties of which were deemed inconsequential in dictating the electrochemical behavior. Hence, detailed advances made in related areas of solid-state and surface physics were not incorporated into electrochemical literature. During the past two decades, however, the basic features of density functional theory (DFT)[4−6] developed for inhomogeneous electron gas at the metal/vacuum interface have been introduced into double-layer studies with suitable modification for solvent dipoles and electrical field effects.[7−11]

The earliest attempt which was made by Rice[12] as early as 1920 to introduce the nature of metal surfaces into electrical double-layer theories was, however, not successful because of the primitive Thomas−Fermi (TF) version employed, with the consequence that this approach remained dormant for more than five decades. However, improvements in this direction were later taken by Kornyshev et al.[13] by applying nonlocal electrostatics to the metal/electrolyte interface. Further progress in this arena has been achieved essentially due to the pioneering work of Badiali,[14] Schmickler and Henderson,[15−17] and Price and Halley.[18−20] While the analysis presented by Schmickler and Henderson and Badiali centered around the description of the metal surface using different versions of the Jellium model, with diverse trial functions for the electron-density profile,[14,21−23] the approach of Price and Halley involves the numerical solution of the Schrodinger equation.[24−26] While the former procedure has simplicity and offers scope for hierarchial improvements, the latter, namely that of Price and Halley, has an inbuilt rigorousness.

The solvent description pertaining to the electrical double layer has also been handled in a variety of ways. In their early work, Badiali et al.[14] considered a continuum dielectric model, while Schmickler[15,16] treated a monolayer of discrete dipoles adsorbed on metal surfaces. In a further significant advance, Badiali,[27] Schmickler and Henderson,[17] and Price and Halley[19,20] have taken the electrolyte to be a solution of hard sphere ions in a dipolar hard sphere solvent. The mean spherical approximation[28] customarily used in this context has recently been improved by Patey et al.[29] with the reference hypernetted chain approximation (RHNC),[30−32] and the Jellium model has been treated following the general self-consistent approach developed by Gies and Gerhardts[33] for metal slabs of finite thickness. Recently, Kinoshita et al.[34] have combined the first principles calculation for the metal surface (replacing the Jellium model) with the RHNC method for the liquid phase across a Pt(111)/H_2O system in a fully self-consistent manner.

Though analysis based on the Jellium model is fairly adequate to describe the general trends observed at the interface for polycrystalline metals, it failed to explain the dependence of double-layer parameters on the various surface planes of metals although carefully estimated experimental data for adsorption of solvent dipoles on single-crystal faces of sp metals exist.[35−38] To overcome this limitation, in recent years, the metal is treated using a modified Jellium model[24−26] in which the discrete nature of the lattice has been taken into account, replacing the uniform background by a lattice of pseudopotentials. This approach has been first introduced into the double-layer problem by Badiali[14] and later by Leiva et al.[39−41] Another approach to double-layer analysis which requires mention here is the development of finite cluster models together with quantum chemical methods of Nazmutdinov et al.[42] to study chemisorption characteristics, in particular, its dependence on the single-crystal face. Although these models differ in finer details, they agree on the basic premise by which the surface electrons influence the double-layer parameters. In addition, they offer a framework in which the electronic effects evidenced by new techniques, such as second harmonic generation (SHG), electroreflectance, scanning

* Author for correspondence.

S1089-5647(98)00371-X CCC: $15.00 © 1998 American Chemical Society
Published on Web 06/05/1998

tunneling microscopy (STM), scanning electrochemical microscopy (SEM), and so forth can also be understood.[1]

The interfacial models discussed above essentially focus upon the calculation of double-layer parameters from molecular models of the solvent and from quantum mechanical models for metals. An alternative strategy is to derive the same parameters by elaborating experimental results on the basis of correlations without involving any specific models. This latter approach, followed by Frumkin[43] and Trasatti,[44] has led to the general characteristics of solvent adsorption at electrodes. The two routes must match somewhere if both are directed to the same end. The existence of one such correlation between the electrochemical properties and the electronic structures of the metal was first mentioned by Frumkin et al.[43] It was suggested that the potential of zero charge (PZC) must be related to the electronic work function of the metal, and this has been extensively discussed in the double-layer literature based on thermodynamic principles.[45] PZC which is an important double-layer parameter at the metal/electrolyte interface has been experimentally obtained from differential capacitance measurements, and much work has been carried out on this by Frumkin et al. for polycrystalline metals and later by Hamelin et al. for single-crystal faces.[45,46] Despite the availability of this quantitative parameter, a detailed theoretical basis for evaluating the same was lacking in the literature until Schmickler[15] postulated a method using microscopic models of the interface. Schmickler's analysis of calculating PZC for polycrystalline metals using the Jellium model for the metal and the monolayer model for treating dipolar interactions using the Langevin function for solvent molecules is inadequate to explain the dependence of PZC on various single-crystal faces of the metal. It is therefore of interest to investigate whether better models for the metal surface as well as for dipolar interactions will yield new insights.

The aim of the present analysis is (i) to estimate the work function for different single-crystal faces of metal, within the modified Jellium model, (ii) to report the face-dependent PZC for sp metals using the work function values, and (iii) to calculate the work function, PZC, and surface potential of water for polycrystalline metals by appropriately averaging over single-crystal faces.

The paper has been organized as follows: Section II deals with the work function calculation at the metal/vacuum interface using a modified Jellium model with pseudopotential effects. In the third section, a brief discussion on the use of the Bethe approximation for the orientational order parameter of solvent dipoles and the evaluation of interfacial parameters at the metal/electrolyte interface using a combination of the Jellium model and the Bethe approximation are given. The discussion of the results is presented in section IV, while section V gives perspectives.

II. Metal/Vacuum Interface and Methodology of Work Function Calculation

The surface electronic properties at the metal/vacuum interface are customarily calculated using DFT formalism founded within the basic theorems of Hohenberg and Kohn.[47,48] It is shown that the ground-state energy of an interacting inhomogeneous electron gas in static external potential can be written as a function of electron density $n(r)$ and the energy attains a minimum for the true $n(r)$ which satisfies the constraint that the total number of electrons in the system is constant. A modified Jellium model, which replaces the positive background charge by a lattice of pseudopotentials, has been used for representing the electron−ion coupling. The electrons are assumed to be distributed smoothly across the ideal boundary, thus protruding toward the exterior and giving rise to a surface dipolar layer. The simplest Ashcroft empty core pseudopotential of the form,[49]

$$\upsilon(r) = 0 \quad \text{if} \quad r < r_c$$

$$= -\frac{Z}{r} \quad \text{if} \quad r \geq r_c \tag{1}$$

has been employed in the present analysis. In eq 1, Z and r_c represent the charge number of the ion and the radius of pseudopotential, respectively. Within r_c, there is perfect cancellation of forces experienced by the electrons at each lattice site. The values of r_c are chosen such that the model reproduces the bulk properties of the metal or that the metal should be stable against changes in density. The surface plane of the metal is situated at a distance $d/2$ in front of the first lattice plane, d being the spacing of lattice planes in the direction perpendicular to the surface. The values d and r_c for the present analysis have been taken from the literature.[26,39] The lattice effect has been introduced as a first-order correction to the Jellium model by Lang and Kohn,[24] but later, Monnier and Perdew[25,26] have used the variational procedure. To keep the model one-dimensional, the pseudopotentials are averaged in the direction parallel to the metal surface. We have employed the procedure followed by Monnier et al.[26] for the pseudopotential contribution to the surface energy. The modified Jellium model has been used to perform calculations for single crystals. It has also been extended to describe sd metals by Russier and Badiali.[50]

Total energy of the electronic plasma is written as a sum of the following terms:

$$E[n(x)] = E_k + E_{xc} + E_{es} + E_{ps} + E_{cl} + E_R \tag{2}$$

The first term is the kinetic energy, which can be written using the gradient expansion as

$$E_k = E_k^{(0)} + E_k^{(1)} \tag{3}$$

where $E_k^{(0)}$ is the Thomas−Fermi contribution and $E_k^{(1)}$ is the second-order density gradient contribution. The second term in eq 2 is the exchange−correlation energy obtained using local density approximation (LDA). Although in recent years, many accurate approximations to this term have been proposed,[51] there is still no way of systematically improving the functional. The third contribution is the surface electrostatic energy, and the last three terms result from the inclusion of lattice of ions. There exist different procedures for the calculation of electronic properties of metals using the above equation.[21−26,51−54] We have followed the method[21] of choosing a suitable family of trial functions for $n(x)$ with several free parameters and then minimizing the surface energy $\sigma(n)^M$, i.e.,

$$\sigma(n)^M = E[n(x)] - E(n) \tag{4}$$

within this family. E_{cl} and E_R which represent the classical cleavage and repulsive energy contributions, respectively, are density-profile independent and, hence, can be eliminated while minimizing the surface energy.

The present model is a modified version of the one originally proposed by Smith[21] for work function calculations, namely, the effect of lattice ions has been taken into account via the Ashcroft pseudopotential term for the electron−ion coupling. The trial function employed in our analysis is

$$n(x) = n(1 - {}^1/_2\, e^{\alpha x})\theta(-x) + {}^1/_2\, n e^{-\alpha x}\theta(x) \qquad (5)$$

where n is the bulk electron density, α is the free parameter which measures the extent of electronic spill-over into the exterior and $\theta(x)$ is the Heaviside step function. The complete expression for the surface energy within the above family of trial functions is given in Appendix 1. Minimization of the surface energy with respect to α subsequently leads to the desired parameters such as work function, surface dipole barrier, and so forth.

The most common method of estimating work function (Φ^M) involves the use of the classical Koopman's Theorem (KT).[55] For the local ion pseudopotential approximation of the lattice[26]

$$\Phi = X - \mu - \langle \delta V \rangle_{av} \qquad (6)$$

where X, the surface potential of the metal, is given by

$$X = \Delta\Phi_M = \phi(\infty) - \phi(-\infty)$$
$$= 4\pi \int_{-\infty}^{\infty} [n(x) - n\theta(-x)]x\, dx \qquad (7)$$

μ is the bulk chemical potential of the electrons relative to the mean electrostatic potential in the metal interior

$$\mu = \frac{\partial(n\epsilon_T)}{\partial n} \qquad (8)$$

where ϵ_T is the sum of kinetic and exchange correlation energies per electron for a uniform electron gas of density n. The pseudopotential contribution $\langle \delta v \rangle_{av}$ is the average value of $\delta v(r)$ over the volume of semiinfinite crystal. In terms of the parameter α, eq 6 takes the form given in Appendix 2 (A2.1).

Work function for polycrystalline surfaces are found to be located in definite positions in the series of values for single-crystal faces depending upon the crystal system under consideration. Hence, these can be obtained using proper averaging procedures over work function of the constituent single-crystal planes. The following equation is used to calculate the work function of polycrystalline samples, namely,[52]

$$\Phi = \sum_i a_i \Phi_i \qquad (9)$$

where a_i is the fraction of the surface occupied by the ith face and Φ_i, the corresponding work function.

III. Dipolar Interactions at Electrochemical Interface Using the Bethe Approximation: Dipole Potential and Potential of Zero Charge

The general features of the present solvent model incorporating the Bethe approximation has been given in detail elsewhere.[56−58] Hence, only a brief discussion of the model is presented here. We consider a two-dimensional discrete lattice of coordination number z whose sites are occupied by solvent dipoles. The dipoles are assigned two configurations designated as "up" (+1) and "down" (−1) orientational states denoting, respectively, the orientation of solvent dipoles with the negative end toward (up) and away (down) from the metal surface. The values +1 and −1 denote the spin variables. The normal components of the permanent dipole moment for up and down orientational states are $-p$ and $+p$, respectively. The dipolar interactions are treated using Bethe approximation, where the interaction of a central dipole with its nearest neighbor dipoles is treated exactly and molecular field approximation (MFA) is used for the interaction of dipoles outside the first shell. The site indices for the central and nearest neighbor dipoles are represented by o and j.

The total Hamiltonian of the system is given by

$$H_T = -pEs_o - p(E + F)\sum_{j=1}^{z} s_j - J\sum_{j=1}^{z} s_o s_j \qquad (10)$$

where the external field $E = 4\pi\sigma^M/\epsilon$, σ^M is the charge density on the metal surface, and ϵ is the dielectric constant of the medium. J, the field due to the interaction of a dipole at site o with that at site j is given by $-p^2/\epsilon z d_s^3$ (the normal component of the permanent dipole moment for the up orientational state is taken as negative and the down orientational state as positive), and d_s is the nearest neighbor distance. The mean field, F, generated by all dipoles outside the central cluster is given by the self-consistent equation

$$\exp\left(\frac{2k_2}{z-1}\right) = \frac{1 + \exp[-2(k_1 + k_2 + \gamma)]}{\exp[-2\gamma] + \exp[-2(k_1 + k_2)]} \qquad (11)$$

where k_1, k_2, and γ are defined as follows

$$k_1 = \frac{pE}{kT}, \quad k_2 = \frac{pF}{kT} \quad \text{and} \quad \gamma = \frac{J}{kT} \qquad (12)$$

In our earlier treatment,[56−58] the contribution of metal to the double-layer structure has been considered in an indirect manner through the introduction of nonelectrostatic interaction energies between the metal and the solvent dipoles to the above Hamiltonian (eq 10). Inadequacy of such a treatment in the double-layer analysis has been indicated by us earlier,[58] and the corresponding terms are now eliminated from eq 10, retaining only the Coulombic contribution for metal−solvent interactions in the total Hamiltonian. Equations 10−12 are formally identical with the Ising Hamiltonian in the context of magnetism.[59,60]

Solving eq 10, the long range order parameter R denoting the net orientation of solvent dipoles, i.e., $(N\uparrow - N\downarrow)/N_T$ (where $N\uparrow$ and $N\downarrow$ are the number of solvent molecules per unit surface area in the up and down orientational states, respectively, and N_T is the total number of solvent molecules), becomes

$$R = \tanh[k_1 + k_2 z/(z-1)] \qquad (13)$$

and the short range order parameter Q defined by $2[(N\uparrow\uparrow + N\downarrow\downarrow) - 2N\downarrow\uparrow]/zN$ (where $N\uparrow\uparrow$, $N\downarrow\downarrow$, and $N\downarrow\uparrow$ are the number of pairs of solvent dipoles in the indicated orientational states) is

$$Q = \frac{\tanh(k_1 + k_2 + \gamma) + \exp(-2[k_1 + k_2 z/(z-1)])\tanh(k_1 + k_2 - \gamma)}{1 + \exp(-2[k_1 + k_2 z/(z-1)])} \qquad (14)$$

The potential drop due to adsorbed solvent dipoles is[56]

$$g_{dip} = -\frac{4\pi N_T p R}{\epsilon} \qquad (15)$$

The above model has also been analyzed including the polarizability effects as well as asymmetry of the dipole moment in the two orientational states.[58] Despite the simplicity, this model has been shown to reproduce satisfactorily the experimental double-layer capacity and its temperature dependence for a set of molecular constants which are obtained through a

nonlinear regression analysis, *provided ad hoc values are employed for metal−solvent interaction energies.*

A metal surface in contact with solution can also be treated with the same concepts as that in a vacuum, if due account is made for possible redistribution of electrons as a result of the presence of a liquid phase. A complete model of the metal/solution interface must describe metal electrons, solvent dipoles, and their interactions in a self-consistent manner. Though it is a formidable task, several attempts have already been made along this line. These emphasize the important role played by the metal electrons but differ considerably in their treatment of the metal−solvent interaction, in particular, the position of the first layer of solvent molecules adjacent to the metal surface. Several groups[19,61] have evaluated the distance of the closest approach between the ionic cores of the metal and the center of solvent molecules (x_1) self-consistently from the molecular interactions at the interface. The parameter x_1 is shown to depend on the type of crystal face and varies with the charge density on the metal surface.[61,62] However, the approach involves uncertainties in the interactions chosen, and the complexity associated with the above calculations makes the error analysis of the parameters a tedious excercise.

In the present framework, we have followed the customary procedure of minimizing interfacial free energy for the metal−solvent coupling[15,16] albeit with certain refinements. Since the correct value of the distance between the metal and the solvent molecules is as yet unknown, we have taken x_1 to be the sum of the crystallographic radius of the metal and the radius of the solvent dipoles,[14] and the variation of x_1 with the crystal faces of the metal has been neglected in our analysis.

The total surface energy at the metal/solution interface now becomes

$$\sigma(n)_{(S)}{}^{M} = \sigma(n)^{M} + \sigma_f(n) \tag{16}$$

where $\sigma(n)^M$ is given by eq 4. The interaction of electrons with the external field (σ_f) is given by

$$\sigma_f = \int_{-\infty}^{x_2} [n(x) - n\theta(-x)] E_{dip} x \, dx$$

$$= \frac{E_{dip} n [1 - \exp(-\alpha x_2)(1 + \alpha x_2)]}{2\alpha^2} \tag{17}$$

where x_2 is the sum of x_1 and the radius of the solvent molecules. E_{dip}, the field due to solvent dipoles adsorbed on the metal surface follows from eq 15 as

$$E_{dip} = -\frac{g_{dip}\theta(x)\theta(x_2 - x)}{x_2} \tag{18}$$

The metal electrons which penetrate into the solution experience both an electrostatic potential and non-Coulombic repulsive potential owing to the interaction with the cores of the solvent dipoles. The repulsive effect is usually represented by a pseudopotential[14,27] or by a potential energy barrier.[17] Inclusion of repulsive potential in the total surface energy of the electronic plasma will add one more adjustable parameter to the model analysis. We have neglected this term in the present analysis, but the interaction of solvent dipoles with the Jellium model has been incorporated in the surface energy minimization.

The total potential drop across the interface is now given by the sum of metal contribution and solvent contribution as

$$\Delta\Phi_T = \Delta\Phi_M{}^{(S)} + \Delta\Phi_{dip} \tag{19}$$

where

$$\Delta\Phi_M{}^{(S)} = 4\pi \int_{-\infty}^{x_2} [n(x) - n\theta(-x)] x \, dx$$

$$= \frac{4\pi n}{\alpha^2} - \frac{2\pi n \exp(-\alpha x_2)}{\alpha^2} - \frac{2\pi n x_2 \exp(-\alpha x_2)}{\alpha} \tag{20}$$

and

$$\Delta\Phi_{dip} = -g_{dip} - \frac{2\pi n x_2 \exp(-\alpha x_1)}{\alpha} \tag{21}$$

If the work function Φ^M, the total potential drop across the interface in the presence, [$\Delta\Phi_T$, cf. eq 19] and absence of solvent, [$\Delta\Phi_M$, cf. eq 7] are known, PZC can be easily obtained through the following thermodynamic relation as[45]

$$PZC = \Phi^M - \Delta\Phi_M + \Delta\Phi_T + E^R \tag{22}$$

where E^R is characteristic of the reference electrode (in the present case, the standard hydrogen electrode) and includes contributions from two terms, namely, the work function of the hydrogen evolution reaction under standard conditions and the potential drop across the surface of the solution which can be estimated from theories of liquids or from energies of solvation and takes the value 4.37 V.[15,45]

IV. Results and Discussion

A. Work Function. The pseudopotential radius r_c, the charge number of the ion Z, and the bulk electron density n for the metals employed in the present analysis are reported in Table 1. The interplanar spacing d for fcc, bcc, and hcp crystal systems are taken from the literature.[26] In Table 2, we present the results for the face-dependent work functions of five sp metals. The polycrystalline work functions are obtained for the four metals by averaging over their single-crystal planes using eq 9. The relative weights of 111, 100, and 110 faces of the metal are 8/25, 5/25, and 12/25, respectively.[63] The bcc crystal system is also averaged using the same fractions as those used for the fcc faces of the metal, since this approximation will lead only to minor error in the analysis compared to that of other approximations employed in the pseudopotential averaging.

According to the Smoluchowski rule,[64] work functions generally increase with increasing packing density. (The most compact faces of fcc and bcc crystal systems are 111 and 110, respectively.) It is clear from the table that the evaluated work functions do show the general trend observed for the two most densely packed crystal faces. Further, the results obtained for polycrystalline metals by averaging over the crystal planes are in good agreement with the experimental data. Although the values pertaining to the 110 face of fcc and the 111 face of bcc crystal systems do not obey the expected trend, this is not surprising in view of the known weakness of the Jellium model while employing trial densities. A more accurate procedure is either to solve the Schrodinger equation itself or to investigate stabilized Jellium models self-consistently using the displaced profile change in the self-consistent field approach, and some progress in this direction has recently been achieved.[65,66] Since our objective is to investigate the variation of PZC as well as that of the dipole potential when electrode surface charge density $\sigma^M = 0$ with single-crystal faces, we do not attempt more refined treatments at this stage.

TABLE 1: Input Parameters for the Present Analysis[a]

metal	n	Z	r_c	R_c[b]
Tl	0.0154	3	1.13	1.98
Pb	0.0196	4	1.12	1.59
Ga	0.0223	3	1.05	1.17
Sn	0.0174	4	1.11	1.40
Zn	0.0195	2	1.27	1.57

[a] n, the bulk electron density; Z, the valence; r_c, the pseudopotential core radius, and R_c, the crystallographic radius. All parameters are given in atomic units. [b] Reference 67.

TABLE 2: Work Functions for Single Crystals and Polycrystalline Samples[a]

metal	crystal face	Φ	polycrystalline Φ	polycrystalline Φ^{II}	polycrystalline Φ^{exp}	face dep Φ literature estimates
Tl	111	4.29				
(fcc)	100	3.39				
	110	3.70				
			3.83	3.45	3.84	
Pb[b]	111	4.79				3.31−4.15
(fcc)	100	3.48				3.45−4.12
	110	3.89				3.72−4.4
			4.10	3.55	4.25	
Ga	111	3.79				
(fcc)	100	3.35				
	110	4.08				
			3.84	3.55	4.2	
Sn	110	4.77				
(bcc)	100	3.47				
	111	4.01				
			4.27	3.57	4.41	
Zn[c]	0001	3.24				4.15−4.3
(hcp)					4.33	

[a] Φ for polycrystalline metals are obtained using two methods of averaging over single crystal planes as described in the text. Φ are obtained by averaging the single crystal values, and Φ^{II} are obtained by averaging the pseudopotential contribution to the surface energy. Φ^{exp} are the experimental work functions. The crystallographic faces for each metal labeled by their Miller indices are arranged from the most to the least densely packed. electronvolts are used for all work function data. [b] References 24, 26, 40, 51−54, 65, 66. [c] References 24, 26, 52, 53, 65, 66.

B. Potential of Zero Charge. The availability of work function estimates is exploited to study the solvent structure at the metal/electrolyte interface. A rigorous approach for obtaining new insights into the organization of solvent dipoles at the interface would be to use both electrochemical and work function data relative to single-crystal faces. As the work functions are face-dependent, so are the PZC values. PZC is a typical property of the given metal/solution interface similar to the electronic work function in the case of a metal surface in a vacuum. Accordingly, PZC depends on the structural details of the electrode surface and is the simplest information one can obtain experimentally about the structure of the electrode/solution interface. Adsorption of neutral molecules such as alcohols is maximum to a first approximation at PZC. For anodic oxidation of some organic compounds as in fuel cells or electro-organic syntheses, a knowledge of PZC is helpful in choosing the appropriate potential ranges. For a rigorous study of corrosion inhibition, a knowledge of PZC is again indispensable since chemisorption of neutral and near-neutral inhibitors are maximum near PZC.

The following procedure has been adopted in our analysis for the theoretical evaluation of PZC.[15] The total surface energy (eq 4) is minimized, and from the value of the free parameter, the net potential drop across the metal/vacuum interface is obtained. The solvent description is then coupled with the metal, and from the new value of α, the potential drop across the metal/solution interface is evaluated using eq 19. Initially, an approximate value of E_{dip} is chosen, and the value of α is obtained by minimizing the energy. The solvent order parameter and the dipolar field are then obtained using the new value of the free parameter. The external field E in the expression for R is taken as the field due to the Jellium model, namely,

$$E = \frac{2\pi n e^{-\alpha x_1}}{\alpha} \tag{23}$$

The total energy is again minimized, and the above steps are repeated until self-consistency is obtained. Substituting the potential drop and work function in eq 22, we obtain PZC. The calculations are limited to sp metals and are not extended to sd and noble metals, since the Jellium model is inadequate to describe the electronic properties of these metals.

TABLE 3: Calculated Potential of Zero Charge for Seven sp Metals Using a Simple Jellium Model (without Pseudopotential) for Metals and the Bethe Approximation for Solvent Dipoles

metal	Φ (eV)	PZC (V) present work[a]	PZC (V) ref 15[b]	PZC (V) exp[44] [c]
Hg	3.33	−1.29	−1.54	−0.193
Ga	3.57	−0.99	−1.43	−0.69
Cd	3.36	−1.26	−1.53	−0.75
In	3.44	−1.17	−1.48	−0.65
Pb	3.50	−1.10	−1.45	−0.56
Sn	3.45	−1.14	−1.48	−0.38
Tl	3.41	−1.21	−1.50	−0.71

[a] Φ in the column are the work functions obtained using smith's trial function for electron-density profile without any modifications in the surface energy. [b] The values of PZC from ref 15 are given for comparison. [c] Experimental data (from ref 44).

First, the theoretical calculations of PZC were carried out for a simple Jellium model without pseudopotential (Table 3). The values show better agreement with experimental data compared to those of mean field analysis for infinite dipolar orientational states.[15] Since the model for the metal is the same in both cases, the improvement in PZC values is attributed to the Bethe approximation for solvent dipoles. As this preliminary analysis gave satisfactory results, we extended our calculations for the evaluation of face-dependent PZC using the work functions given in Table 2, and the results are presented in Table 4. The polycrystalline values are obtained using the same averaging procedure as outlined before for work function calculations (cf. eq 9). The double-layer parameters employed in our analysis are as follows: the distance of closest approach of the solvent to the metal surface, $x_1 = R_c + d_s/2$, where d_s is the diameter of the solvent dipoles $= 3 \times 10^{-10}$ m (R_c values for the metals are given in Table 1), $x_2 = R_c + d_s$, the dipole moment, $p = 6.13 \times 10^{-30}$ cm, the total number of solvent molecules per unit surface area, $N_T = 1 \times 10^{19}$ molecules m^{-2}, the coordination number, $z = 6$, and the inner layer dielectric constant, $\epsilon = 6$. From Table 4, it follows that the PZC values for polycrystalline surfaces give satisfactory agreement with the experimental data and show improvement over existing values. Since no reliable experimental data pertaining to PZC for different single-crystal faces has yet been reported, we are unable to compare our estimates. Nevertheless, a strong dependence of PZC on the type of single-crystal faces does emerge from our analysis and is an interplay of metal/vacuum work functions and dipolar organization. The large difference observed in PZC values between the crystal planes of the metal is due to the work function expression employed in the present analysis.

TABLE 4: Theoretical PZC Values for Single-Crystal Faces and Polycrystalline Metals

			polycrystalline		
metal	face	PZC	PZC[a]	PZC^{II} [b]	PZC^{exp} [c]
Tl	111	−0.34			
(fcc)	100	−1.24			
	110	−0.91			
			−0.79	−1.17	−0.71
Pb	111	0.16			
(fcc)	100	−1.14			
	110	−0.66			
			−0.49	−1.06	−0.56
Ga	111	−0.82			
(fcc)	100	−1.25			
	110	−0.13			
			−0.57	−1.02	−0.69
Sn	110	0.14			
(bcc)	100	−1.12			
	111	−0.09			
			−0.18	−1.03	−0.38
Zn	0001	−1.38			
(hcp)					

[a] PZC for polycrystalline metals obtained by averaging over single-crystal estimates. [b] Pseudopotential contributions to the surface energy. [c] Experimental PZC values for polycrystalline metals are also tabulated. All PZC values are reported in volts.

TABLE 5: Calculated Surface Potentials of Water by Averaging over the Single-Crystal Planes

metal	$\Delta\Phi_{dip}$ (V)	$\Delta\Phi_{dip}$[a] (V)
Tl	0.10	0.20
Pb	0.17	0.19
Ga	0.30	0.33
Sn	0.22	0.14
Zn	0.07	0.32

[a] The surface potentials derived from experimental data by Trasatti.[45]

Better estimates of PZC can be obtained by employing displaced profile change in the self-consistent field[53] procedure for the calculation of work functions.

An alternative method of obtaining work function and potential of zero charge for polycrystalline metals directly without using PZC values for the single-crystal planes has also been analyzed. In this case, the pseudopotential contribution to the surface energy itself (A1.6) is averaged over single-crystal planes. The results are shown in column 5 of Tables 2 and 4. It is obvious from the calculations that the results obtained using the first procedure where estimates for various crystal faces are averaged to obtain values for polycrystalline metals are superior to the alternate method of averaging.

C. Dipole Potential and Order Parameters at PZC. At the potential of zero charge, there is a preferred orientation of solvent dipoles at electrochemical interfaces. To obtain the theoretical estimate for this parameter, we have employed in our earlier analysis[57] an adjustable parameter which takes into account the nonelectrostatic interactions of the solvent dipoles with the metal surface. Such an ad hoc introduction is, however, not necessary as the metal−solvent coupling can be obtained directly from the Jellium model of the metal surface. Table 5 summarizes the values of the surface potential of water calculated by using eq 21, along with the values given by Trasatti.[45] The positive sign of the surface potential obtained corresponds to dipoles with the oxygen atom pointing to the metal surface. The dipole potentials in our analysis are again the mean values determined by the proportions of the respective planes present on a polycrystalline surface. The model employed here for the calculation of surface potential differs from that of Schmickler,[17]

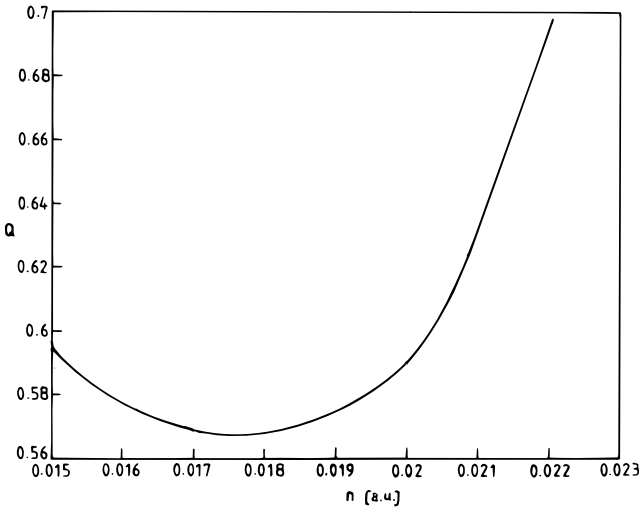

Figure 1. Variation of short-range-order parameter of solvent dipoles with bulk electron density of metals.

who employed mean field analysis for the infinite state solvent dipoles and the Jellium model without a pseudopotential for the metal. In contrast to models based on molecular field approximation where local correlations are ignored, the Bethe approximation provides a basis for incorporating them. In view of this, it is imperative to determine the variation of the short-range-order parameter Q with respect to the electronic properties of metals. Hence, we have evaluated Q from eq 14 self-consistently, as in the case of PZC, for fcc and bcc polycrystalline metals. Figure 1 indicates that short-range ordering is in fact influenced by the nature of the metal surfaces. We reiterate that this dependence of the short-range-order parameter of solvent dipoles on electron density of the metals reported here, using discrete models, is hitherto unknown.

V. Perspectives

In recent years, hard sphere electrolyte models have improved our comprehension of double-layer structure at the metal/solution interface. The complexity associated with the continuum models makes the extension to nonzero electric fields tedious and thus requires an elaborate treatment. The present analysis assumes a sharp boundary between the inner and the diffuse layer at the metal/electrolyte interface. Despite the criticism associated with the artificial division of double-layer models, the monolayer models for solvent dipoles with a proper quantum mechanical model for the metal surface offer simplicity and provide scope for hierarchial improvements and can also be extended to other charge densities without extensive numerical calculations. A simple one-parameter family of trial functions for the electron-density profile is used to solve the modified Jellium model, and the face-dependent work functions and PZC are obtained for five sp metals, for which reliable electrochemical experimental data pertaining to polycrystalline samples exist. The calculated surface properties for single crystals agree with the experimental trend for the two most densely packed surface planes. The sophisticated quantum mechanical models developed recently for metal surfaces, such as the structureless pseudopotential model[65] employing trial functions for the electron-density profile, have also not been successful in predicting the correct face-dependence of surface parameters for all three planes of higher density metals. The present analysis assumes polycrystalline samples to be composed of certain fractions of various single-crystal faces, and the values are obtained through averaging over their crystal planes. Two

methods of averaging are employed. The second procedure (where the pseudopotential contribution to the surface energy is averaged) gives low estimates of work function and, hence, leads to poor agreement for PZC values. The other averaging procedure employed here (where the appropriate parameters for single-crystal faces are first obtained and subsequently averaged) predicts more accurate values for the work function and PZC of polycrystalline metals. Although the PZC estimates for polycrystalline metals do not show good agreement with the experimental data, the present analysis indicates the scope for more involved procedures for evaluating the structure of electrochemical interfaces along the following directions in the future, namely, (i) different choices of trial functions, and incorporation of Friedel oscillations, (ii) various pseudopotential forms and their influence on interfacial properties, (iii) more involved averaging procedures to obtain polycrystalline values from single-crystal estimates, and (iv) inclusion of $\infty-$state dipolar models which go beyond the Bragg−Williams approximation as well as the Bethe approximation.

Summary

An extended Jellium model which incorporates the effect of lattice ions in the form of the Ashcroft pseudopotential term has been analyzed for obtaining estimates of the work functions for single crystals and polycrystalline metals. The present approach yields satisfactory values for work functions at the metal/vacuum interface for polycrystalline metals. The Bethe approximation for solvent dipoles is then coupled with the model for the metal surface and employed to obtain PZC and the surface potential of water at $\sigma^M = 0$.

Appendix 1

For the trial density given by eq 5, the following expressions represent different contributions to the surface energy. The kinetic energy

$$\sigma_k = -\frac{3}{10}(3\pi^2)^{2/3}\frac{n^{5/3}}{\alpha}(0.572) + \frac{\alpha n}{72}\ln 2 \qquad \text{(A1.1)}$$

Exchange−correlation energy has the form

$$\sigma_{xc} = \frac{3}{4}\left(\frac{3}{\pi}\right)^{1/3}\frac{n^{4/3}}{\alpha}(0.339) - \frac{I(n)}{\alpha} - \frac{0.084n}{\alpha}\left(a^2 - \frac{1}{2}a + \frac{1}{3} + a^3\ln\frac{a}{a+1}\right) \qquad \text{(A1.2)}$$

where

$$I(n) = \frac{0.168n}{1+k}\int_{2^{-1/3}}^{1}\frac{(1+k)x^4 - (x+k)}{(x+k)(1-x^3)}x^2\,dx \qquad \text{(A1.3)}$$

The above integral can also be evaluated analytically.[11] k and a in eq A1.3 are given by

$$k = \frac{0.079}{n^{1/3}} \qquad \text{and} \qquad a = 2^{1/3}k \qquad \text{(A1.4)}$$

The electrostatic part is,

$$\sigma_{es} = \frac{\pi n^2}{2\alpha^3} \qquad \text{(A1.5)}$$

and the pseudopotential contribution becomes

$$\sigma_{ps} = \frac{2\pi n^2 d}{\alpha^2}\left(\frac{1}{\alpha d} - \frac{\cosh(\alpha r_c)}{2\sinh(\alpha d/2)}\right) \qquad \text{(A1.6)}$$

Equations A1.1 to A1.6 are well-known.[54]

Appendix 2

The expression for the work function using the trial density employed here is given as

$$\Phi = \frac{4\pi n}{\alpha^2} - \frac{(3\pi^2 n)^{2/3}}{2} + \left(\frac{3n}{\pi}\right)^{1/3} + \frac{0.056n^{2/3} + 0.0059n^{1/3}}{(0.079 + n^{1/3})^2} + \frac{Zd^2}{8r_0^3}\left(1 - \frac{12r_c^2}{d^2}\right) \qquad \text{(A2.1)}$$

where

$$r_0^3 = \frac{3Z}{4\pi n} \qquad \text{(A2.2)}$$

References and Notes

(1) Schmickler, W. *Chem. Rev.* **1996**, *96*, 3177.
(2) Rangarajan, S. K. In *Specialist Periodical Reports: Electrochemistry*; Thrisk, H. R., Ed.; The Chemical Society: London, 1980.
(3) Guidelli, R. In *Trends in Interfacial Electrochemistry*; Silva, A. F., Ed.; Reidel: Dordrecht, 1986.
(4) Rajagopal, A. K. *Adv. Chem. Phys.* **1980**, *41*, 59.
(5) Parr, R. G.; Yang, W. *Density Functional Theory of Atoms and Molecules*; Oxford University Press: New York, 1989.
(6) Kohn, W.; Becke, A. D.; Parr, R. G. *J. Phys. Chem.* **1996**, *100*, 12974.
(7) Schmickler, W. In *Trends in Interfacial Electrochemistry*; Silva, A. F., Ed.; Reidel: Dordrecht, 1986; p 453.
(8) Schmickler, W.; Henderson, D. *Prog. Surf. Sci.* **1986**, *22*, 323; Schmickler, W. In *Structure of Electrified Interfaces*; Lipkowski, J., Ross, P. N., Ed.; VCH Publishers: New York, 1993; p 201.
(9) Kornyshev, A. A. *Electrochim. Acta* **1989**, *34*, 1829; Kornyshev, A. A. In *Condensed Matter Physics Aspects of Electrochemistry*; Tosi, M. P., Kornyshev, A. A., Eds.; World Scientific: Singapore, 1991; p 7; Kornyshev, A. A.; Kuznetsov, A. M.; Makov, G.; Vigdorovitch, M. V. *J. Chem. Soc., Faraday Trans.* **1996**, *92*, 3997; 4005.
(10) Badiali, J. P. *Electrochim. Acta* **1986**, *31*, 149; Badiali, J. P.; Amokrane, S. In *Condensed Matter Physics Aspects of Electrochemistry*; Tosi, M. P., Kornyshev, A. A., Eds.; World Scientific: Singapore, 1991; p 157; Amokrane, S.; Badiali, J. P. In *Modern Aspects of Electrochemistry*; Conway, B. E., White, R. E., Bockris, J. O'M., Eds.; Plenum Press: New York, 1992; Vol. 22, p 1.
(11) Henderson, D. In *Trends in Interfacial Electrochemistry*; Silva, A. F., Ed.; Reidel: Dordrecht, 1986.
(12) Rice, O. K. *Phys. Rev.* **1928**, *30*, 1051.
(13) Kornyshev, A.; Schmickler, W.; Vorotyntsev, M. *Phys. Rev.* **1982**, *B25*, 5244.
(14) Badiali, J. P.; Rosinberg, M. L.; Goodisman, J. *J. Electroanal. Chem.* **1981**, *130*, 31; **1983**, *143*, 73; 1983, *150*, 25.
(15) Schmikler, W. *Chem. Phys. Lett.* **1983**, *99*, 135.
(16) Schmickler, W. *J. Electroanal. Chem.* **1983**, *150*, 19.
(17) Schmickler, W.; Henderson, D. *J. Chem. Phys.* **1984**, *80*, 3381; **1985**, *82*, 2825; **1986**, *85*, 1650.
(18) Price, D.; Halley, J. W. *J. Electroanal. Chem.* **1983**, *150*, 347; Halley, J. W.; Johnson, B.; Price, D.; Schwalm, M. *Phys. Rev.* **1985**, *B31*, 7695.
(19) Halley, J. W.; Price, D. *Phys. Rev.* **1987**, *B35*, 9095; **1988**, *B38*, 9357.
(20) Price, D. L.; Halley, J. W. *J. Chem. Phys.* 1995, *102*, 6603.
(21) Smith, J. R. *Phys. Rev.* **1969**, *181*, 522.
(22) Partenskii, M.; Smorodinskii, Ya. *Sov. Phys. Solid State (Engl. Transl.)* **1974**, *16*, 423.
(23) Schmickler, W.; Henderson, D. *Phys. Rev.* **1984**, *B30*, 3081.
(24) Lang, N. D.; Kohn, W. *Phys. Rev.* **1970**, *B1*, 4555; **1971**, *B3*, 1215; **1973**, *B8*, 6010.
(25) Perdew, J. P.; Monnier, R. *Phys. Rev. Lett.* **1976**, *37*, 1286.
(26) Monnier, R.; Perdew, J. P. *Phys. Rev.* **1978**, *B17*, 2595.
(27) Badiali, J. P.; Rosinberg, M. L.; Vericat, F.; Blum, L. *J. Electroanal. Chem.* **1983**, *158*, 253.
(28) Carnie, S. L.; Torrie, G. M. *Adv. Chem. Phys.* **1984**, *56*, 141.

(29) Berard, D. R.; Kinoshita, M.; Ye, X.; Patey, G. N. *J. Chem. Phys.* **1994**, *101*, 6271.
(30) Berard, D. R.; Patey, G. N. *J. Chem. Phys.* **1991**, *95*, 5281.
(31) Wei, D.; Torrie, G. M.; Patey, G. N. *J. Chem. Phys.* **1993**, *99*, 3990 and references therein.
(32) Kinoshita, M.; Harada, M. *Mol. Phys.* **1994**, *81*, 1473.
(33) Gies, P.; Gerhardts, R. R. *Phys. Rev.* **1986**, ***B33***, 982.
(34) Yamamoto, M.; Kinoshita, M. *Chem. Phys. Lett.* **1997**, *274*, 513.
(35) Valette, G.; Hamelin, A. *J. Electroanal. Chem.* **1973**, *45*, 301.
(36) Hamelin, A.; Titanov, T.; Sevastinov, E.; Popov, A. *J. Electroanal. Chem.* **1983**, *145*, 225.
(37) Valette, G. *J. Electroanal. Chem.* **1981**, *122*, 285; **1982**, *183*, 37.
(38) Hamelin, A. *J. Electroanal. Chem.* **1992**, *329*, 247.
(39) Leiva, E.; Schmickler, W. *J. Electroanal. Chem.* **1986**, *205*, 323.
(40) Leiva, E. *Chem. Phys. Lett.* **1991**, *187*, 143.
(41) Leiva, E.; Schmickler, W. *Surf. Sci.* **1993**, *291*, 226.
(42) Nazmutdinov, R. R.; Probst, M.; Heinzinger, K. *Chem. Phys. Lett.* **1994**, *221*, 224. Nazmutdinov, R. R.; Shapnik, M. S. *Electrochim. Acta* **1996**, *41*, 2253.
(43) Frumkin, A. N.; Petrii, O. A.; Damaskin, B. B. In *Comprehensive Treatise of Electrochemistry*; Bockris, J. O'M., Conway, B. E., Yeager, E., Eds.; Plenum Press: New York, 1980; Vol.1.
(44) Trasatti, S. In *Trends in Interfacial Electrochemistry*; Silva, A. F., Ed.; Reidel: Dordrecht, 1986.
(45) Trasatti, S. In *Advances in Electrochemsitry and Electrochemical Engineering*; Gerischer, H., Tobias, C. W., Eds.; Wiley Interscience: New York, 1977; Vol. 10, p 213.
(46) Hamelin, A. In *Trends in Interfacial Electrochemistry*; Silva, A. F., Ed.; Reidel: Dordrecht, 1986.
(47) Hohenberg, P.; Kohn, W. *Phys. Rev.* **1964**, *136*, B864.
(48) Kohn, W.; Sham, L. J. *Phys. Rev.* **1965**, *140*, A1133.
(49) Ashcroft, N. W. *Phys. Lett.* **1966**, *23*, 48.
(50) Russier, V.; Badiali, J. P. *Phys. Rev.* **1989**, *B39*, 13193.
(51) Perdew, J. P.; Zhang, Z. Y.; Langreth, D. C. *Phys. Rev.* **1990**, *B41*, 5674; for a recent review of the different exchange correlation functionals, see, e.g., Neumann, R.; Nobes, R. H.; Handy, N. C. *Mol. Phys.* **1996**, *87*, 1.
(52) Sahni, V.; Perdew, J. P.; Grunebaum, J. *Phys. Rev.* **1981**, *B23*, 6512.
(53) Monnier, R.; Perdew, J. P.; Langreth, D. C.; Wilkins, J. W. *Phys. Rev.* **1978**, *B18*, 656.
(54) Keijna, A. *J. Phys. C: Solid State Phys.* **1982**, *15*, 4717.
(55) Koopmans, T. *Physica* **1933**, *1*, 104.
(56) Saradha, R.; Sangaranarayanan, M. V. *J. Chem. Phys.* **1996**, *105*, 4284.
(57) Saradha, R.; Sangaranarayanan, M. V. *J. Colloid Interface Sci.* **1996**, *183*, 610.
(58) Saradha, R.; Sangaranarayanan, M. V. *Langmuir* **1997**, *13*, 5470.
(59) Kubo, R. *Statistical Mechanics*; Elsevier Science Publishers, B. V.: New York, 1965; chapter 5.
(60) Plischke, M.; Bergensen, B. *Equilibrium statistical physics*; Prentice Hall: New York, 1989; chapter 3.
(61) Amokrane, S.; Badiali, J. P. *Electrochim. Acta* **1989**, *34*, 39; *J. Electroanal. Chem.* **1989**, *159*, 315.
(62) Feldman, V. I.; Kornyshev, A. A.; Partenskii, M. B. *Solid State Commun.* **1985**, *53*, 157.
(63) Valette, G.; Hamelin, A. *J. Electroanal. Chem.* **1973**, *45*, 301.
(64) Smoluchowski, R. *Phys. Rev.* **1941**, *60*, 661.
(65) Perdew, J. P.; Tran, H. Q.; Smith, E. D. *Phys. Rev.* **1990**, *B42*, 11627.
(66) Keijna, A. *Phys. Rev.* **1993**, *B47*, 7361.
(67) Animalu, A. O. E.; Heine, V. *Philos. Mag.* **1965**, *12*, 1249.